

# Simplified Approach to Model Steel Rebar-Concrete Interface in Reinforced Concrete

Rashid Hameed\*, Alain Sellier\*\*, Anaclet Turatsinze\*\*\*, and Frédéric Duprat\*\*\*\*

Received May 21, 2015/Revised December 29, 2016/Accepted April 26, 2016/Published Online July 27, 2016

## Abstract

For correct description of cracking process in reinforced concrete structural elements, the simulation of the behaviour of steel rebar-concrete interface is always of primary importance. This paper proposes a simplified method to model the steel rebar-concrete interface in RC structures. The proposed method considers the introduction of massive elasto-plastic isotropic bond element as steel rebar-concrete interface. Stress-strain behaviour curve required for elasto-plastic isotropic material is obtained by performing conventional pull-out tests on concrete. For plain concrete matrix, an orthotropic damage model based on plasticity and damage theories was adopted for finite element modelling in Finite Element (FE) code CASTEM. In order to validate the proposed approach, a comprehensive experimental program was designed and carried out. Under this program, pure tension test on RC prisms and flexural test on RC beams were performed. Testing of proposed steel rebar-concrete interface bond model in numerical simulation of RC prism subjected to pure tension and RC beam in flexure, and comparison of numerical simulation results with experimental data is also discussed in this paper.

Keywords: RC, steel rebar-concrete interface, elasto-plastic isotropic element, numerical simulation, FEM code CASTEM

## 1. Introduction

Strength, stiffness, efficiency and economy of Reinforced Concrete (RC) make it most widely used construction material in the whole world. Utility of RC, being the most widely used material is derived from the combination of two materials; concrete matrix which is strong and durable in compression and steel which is strong and ductile in tension. In order to maintain composite action between two materials, transfer of stresses between them through bond is essential (Dominguez and Ibrahimbegovic, 2006; Wang and Liu, 2003).

In predicting the behaviour of RC structures close to reality, consideration of bond-slip phenomenon is must (Jendele and Cervenka, 2006; Mazzarolo *et al.*, 2012). Currently, various numerical models are available to represent the steel-concrete bond behaviour. Among them, some models consider the introduction of zero thickness elements at steel-concrete interface (Casanova *et al.*, 2012). In the past, a spring element to relate the steel and concrete nodes was also proposed by Ngo and Scordelis (1967). Many research studies have been carried out to simulate the behaviour of reinforced concrete structural elements

taking into account behaviour of bond between concrete and steel rebar such as model based on plasticity theory (Cox and Guo, 2000) or the damage theory (Ragueneau *et al.*, 2006; Willam *et al.*, 2004) but few studies were focused on the role of interface between concrete and rebar in the cracking process of the concrete.

In recent years, different finite elements have been proposed to model the bond effects in RC structures (Radtko *et al.*, 2010). The models which are based on interface elements (joint elements) are more difficult to use because they need an oriented mesh of the interface with a volume description of the bar which costs more in terms of computation resources and time. Recently a new bond slip model for reinforced concrete structures has been proposed by Mang *et al.* (2015). This type of model needs an intensive modifications of FE code (new element type not simply constitutive law), as it is not allowed in all commercial codes. Considering this kind of restrictions, an approach based on plastic interface presents a practical interest.

In this contribution, an approach to model the steel-concrete interface by introducing massive bond element with elasto-plastic isotropic behaviour is proposed. Experimental pull-out

\*Associate Professor, Civil Engineering Dept., University of Engineering and Technology Lahore, Pakistan (Corresponding Author, E-mail: rashidmu-ghal@uet.edu.pk)

\*\*Professor, Université de Toulouse; UPS-INSa; LMDC (Laboratoire Matériaux et Durabilité des Constructions); 135 avenue de Rangueil; F-31077 Toulouse Cedex 04, France (E-mail: alain.sellier@insa-toulouse.fr)

\*\*\*Professor, Université de Toulouse; UPS-INSa; LMDC (Laboratoire Matériaux et Durabilité des Constructions); 135 avenue de Rangueil; F-31077 Toulouse Cedex 04, France (E-mail: anaclet.turatsinze@insa-toulouse.fr)

\*\*\*\*Professor, Université de Toulouse; UPS-INSa; LMDC (Laboratoire Matériaux et Durabilité des Constructions); 135 avenue de Rangueil; F-31077 Toulouse Cedex 04, France (E-mail: frederic.duprat@insa-toulouse.fr)

test is always considered to be the main tool which provides necessary information required for modelling of bond between steel and concrete (Pyo and Lee, 2010). Stress–strain behaviour curve required for elasto-plastic material model was obtained through performing pull-out tests on concrete samples as per RILEM Standards (RILEM 7-II-128, 1994). After description of the proposed bond element, its validation through uni-axial pure tensile loading test on RC prism and flexure tests on RC beam is discussed in this paper. The finite element code CASTEM (Cast3M, 2000) is used to perform finite element analysis. The detail description of the FEM code CASTEM and as well as detailed theoretical formulation of used damage model of concrete is not the purpose of this paper. The latter has already been published (Sellier *et al.*, 2012a; Sellier *et al.*, 2012b).

## 2. Model Presentation

Reinforced Concrete (RC) is modelled as three phase material; 1) massive concrete with cubic elements and damage model; 2) steel-concrete interface with cubic elements and elasto-plastic model; and 3) and uni-axial bar element with cross sectional area and material properties same as that of steel bar.

### 2.1 Interface Element

The method adopted to model the interface between steel reinforcing bars and concrete is schematically shown in Fig. 1, where it can be noticed that the area of the steel bar is replaced by an interface bond element assembly which is square in shape to simplify its integration in finite element mesh based on cubic elements, but both side dimension deduced from the diameter of the steel bar to conserve the global stiffness of the reinforced concrete. In order to keep the global stiffness of the composite same in the elastic range for the two cases shown in Fig. 2,  $\alpha$  is defined as the ratio between elastic modulus of the interface bond element  $E_i$  and elastic modulus of massive concrete  $E_c$ . The behaviour law used for this interface was elasto-plastic but with a multi-nonlinear yielding curve deduced from a pull-out test as shown in Fig. 3.

Let the global stiffness of the two equivalent systems shown in Fig. 2 is  $K_o$ , combined stiffness of the two phase system shown in Fig. 2 (on left) and three phase system in Fig. 2 (on right) is given in Eq. (1) and Eq. (2), respectively.

$$E_c(A_c - A_s) + E_{ss}A = K_o \quad (1)$$

$$E_c(A_c - A_i) + E_iA_i + E_sA_s = K_o \quad (2)$$

By equating Eqs. (1) and (2), we obtain;

$$E_c(A_c - A_s) + E_sA_s = E_c(A_c - A_i) + E_iA_i + E_sA_s \quad (3)$$

From the Eq. (3), expression for the ratio of elastic modulus of interface bond element and massive concrete is obtained as;

$$\frac{E_i}{E_c} = 1 - \frac{A_s}{A_i} \Leftrightarrow \alpha = 1 - \frac{A_s}{A_i} \quad (4)$$

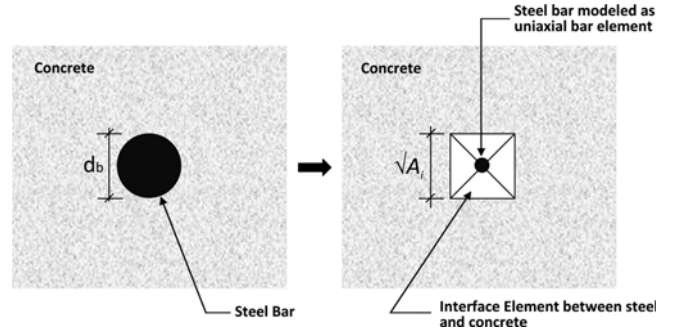


Fig. 1. Method to Model Interface between Steel Rebar and Concrete

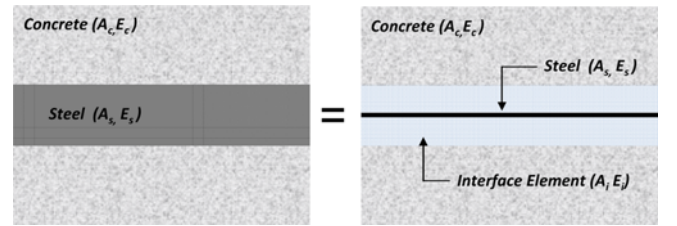


Fig. 2. Global Stiffness of Two Equivalent Systems

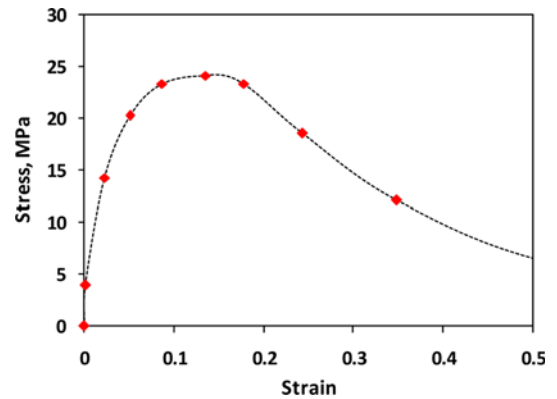


Fig. 3. Uni-axial Multi-linear Hardening Curve used to Model Interface Bond Element

Consequently the section of the interface element has to be chosen as a function of alpha.

$$A_i = \frac{A_s}{1 - \alpha} \quad (5)$$

It is important to mention here that shear modulus is also a fitting parameter needed to control initial shear stiffness of the interface independently of the axial modulus computed as explained in Eqs. (1) to (5). The plastic criterion used in the interface is based on von Mises one, without dilatancy but with the non linear hardening curve shown in Fig. 3. In the interface zone, the constitutive behaviour law is  $\sigma = S(\varepsilon - \varepsilon^{pl})$  and  $\varepsilon^{pl}$  is the interface plastic strain derived from the standard plasticity theory based on von Mises criterion with the non linear hardening, which is a very robust plastic law. The plastic dissipation during sliding takes place in a controlled volume depending on the reinforcement diameter. The correct dissipation is obtained by a

direct fitting of the plastic hardening law on a pull out test (inverse analysis).

### 2.2 Plain Concrete Model

The plain concrete behaviour is modelled with an orthotropic damage model (Sellier *et al.*, 2012a; Sellier *et al.*, 2012b). The model is based on plasticity and damage theories. The principle of the model consists of computing first an effective stress  $\vec{\sigma}$  depending on the total strain  $\vec{\varepsilon}$  and plastic strain  $\vec{\varepsilon}^p$  (Eq. 6):

$$\vec{\sigma} = \mathcal{S}^0 \cdot (\vec{\varepsilon} - \vec{\varepsilon}^p) \quad (6)$$

Where,  $\mathcal{S}^0$  is the stiffness matrix of the undamaged material,  $\vec{\varepsilon}^p$  is the plastic strain which is the sum of two types of strains (Eq. 7)

$$\vec{\varepsilon}^p = \vec{\varepsilon}^t + \vec{\varepsilon}^c \quad (7)$$

$\vec{\varepsilon}^t$  corresponds to the plastic strain associated with the localised tensile cracks, and  $\vec{\varepsilon}^c$  the plastic strains associated with the shear phenomena. As the effective stresses  $\vec{\sigma}$  are representative of stress state in the undamaged part of the material, they are linked to the apparent stresses using a classical damage formulation (Eq. 8) in which the positive effective stresses ( $\vec{\sigma}^t$ ) and the negative effective stresses ( $\vec{\sigma}^c$ ) play a different role, depending if the tensile cracks represented by the damage variables  $\mathcal{D}^t$  are opened or closed.

$$\vec{\sigma} = (1 - \mathcal{D}^c) \cdot (1 - \mathcal{D}^t) \cdot \vec{\sigma}^t + (1 - \mathcal{D}^c) \cdot \vec{\sigma}^c \quad (8)$$

Tensile damage  $\mathcal{D}^t$  and compressive damage  $\mathcal{D}^c$  are functions of plastic strains. In fact, two damage mechanisms are assumed in this model; first one is dedicated to the tensile crack, it is based on main tensile stresses criteria, and a second one to the crushing, based on a Drucker Prager criterion. But, as plastic strains are also associated to these mechanisms, it is possible to link directly the damage variable to the plastic strains. Fig. 4 shows the different criteria from which plastic strains are derived. As there are two types of criteria, there are two types of plastic strains and two types of damages. The tensile plastic strains ( $\vec{\varepsilon}^t$ ) are derived from the orthotropic Rankine criteria

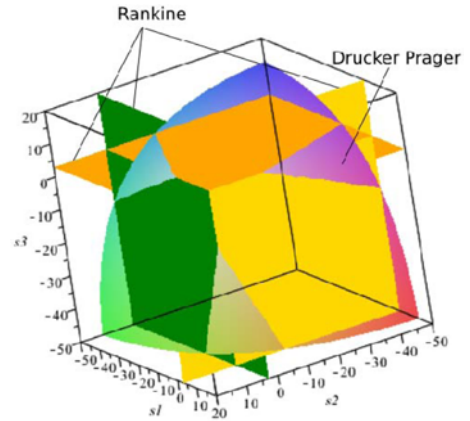


Fig. 4. Plastic Criteria in Principal Stresses Base (Sellier, 2015)

while compression/shear plastic strains ( $\vec{\varepsilon}^c$ ) are derived from a Drucker Prager criterion. The detail of each criterion is classical and has already been published in (Sellier *et al.*, 2012a). For the Rankine criteria, the plastic flow rules used to compute  $\vec{\varepsilon}^t$  corresponds to a standard formulation (associated formulation i.e., the criteria and the plastic potential are the same function), while in compression a non-standard formulation is used to control the dilatency induced by the evolution of  $\vec{\varepsilon}^c$  (the plastic potential is a Drucker Prager function with a different internal friction coefficient then in the criterion). The originality of the model lies in the fact that, in tension, as in compression, the criteria are not computed with the real stresses but with the effective stresses defined as the stresses in the undamaged part of the material (Eq. (6)). That is why the initial stiffness matrix  $\mathcal{S}^0$  is used for the plastic sub-problem (instead of the damaged stiffness matrix). The hardening laws used in the effective stress space are very simple since they correspond to a perfect plasticity. So the post peak softening of the behaviour law as illustrated in Fig. 5 is the consequence of damage, not only of the plasticity.

Both damages are increasing functions of the plastic strains ( $\vec{\varepsilon}^t$  and  $\vec{\varepsilon}^c$  respectively). These functions are chosen in such a

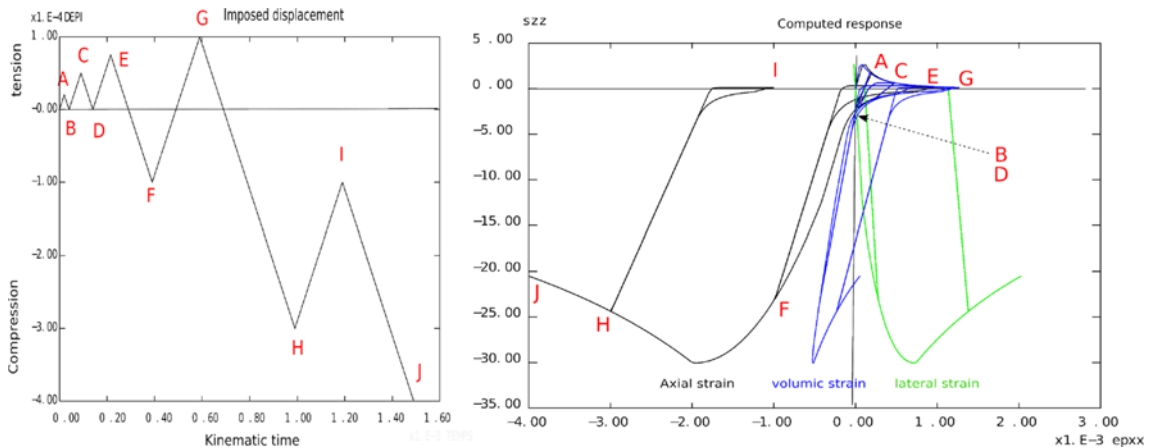


Fig. 5. Plain Concrete Model Response under Uniaxial Cyclic Loading (Sellier, 2015)

way that the fracture energy  $G_f$  is dissipated in a finite element when the tensile damage reaches the unit value. In compression, the function is in relation with the plastic dilatency, more the plastic strain volumic variation, more the compressive damage.

As the Rankine criteria are orthotropic, the plastic strain and the tensile damage is a second order tensor affecting each main effective stress differently. The orthotropic damage formulation on which the plain concrete model is based allows using an orthotropic Hillerborg method, and consequently ensures the objectivity of the FEM analysis toward the mesh size. The plastic formulation allows a hysteretic dissipation due to tensile crack re-closing as illustrated in Fig 5. This model also allows computing the tensile crack opening which can be plotted on the finite element mesh of specimen.

The thermodynamic justification of the damage model is already published in (Sellier *et al.*, 2012a) and it has been shown that the dissipation is always positive whatever is the loading pass, and allows controlling the fracture energy released during the tensile damage increase independently of the mesh size thanks to the anisotropic variant of the Hillerborgh method.

### 2.3 Behaviour Law of Steel Reinforcing Bars

An elastic perfectly plastic behaviour law is used to model the steel reinforcing bars in this study. In most of the commercially available finite element codes, this type of behaviour law for steel reinforcing bars is generally available.

## 3. Model Fitting and Validation

In this part of the paper, fitting and validation of the method proposed to model the interface between steel reinforcing bars and concrete matrix for reinforced concrete element is carried out. For this purpose, three different types of tests are simulated: pull-out test on cubic specimen for model fitting and pure tensile uniaxial loading test on prismatic specimen and three point bending tests on RC beam for model validation. For fitting and validation of the proposed approach for steel rebar-concrete interface modelling, finite element code CASTEM (Cast3M, 2000) was employed.

### 3.1 Fitting of Model Parameters

Fitting of different model parameters was performed through simulating the pull-out test. Three dimensional finite element mesh of the pull-out test specimen made in CASTEM is shown Fig. 6 which provides all necessary information about the boundary conditions and symmetrical surfaces. In the simulation of pull-out test, considering the double symmetry of the problem one fourth of the specimen is modelled to reduce the computation time. The values of different model parameters given in Table 1 to Table 3 were obtained through experiments.

Fitted load versus slip response from the numerical modelling was compared with experimental data and is presented in Fig.7.

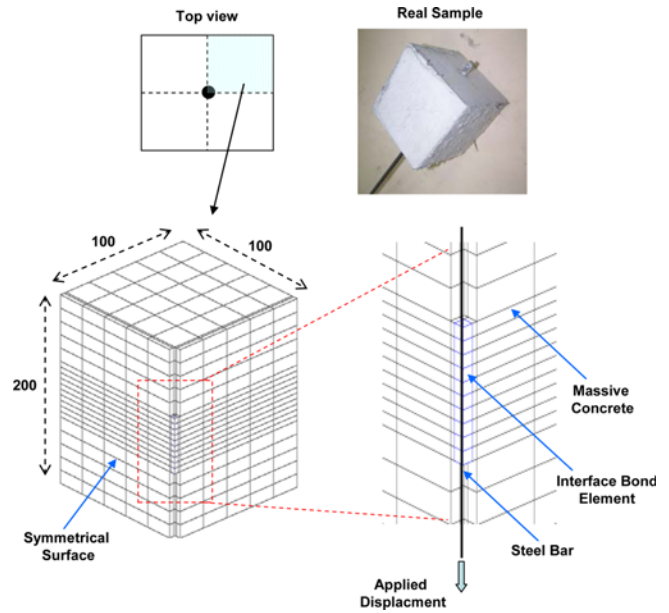


Fig. 6. 3D Finite Element Mesh of one Fourth of Pullout Test Specimen

Table 1. Parameters of Damage Model for Massive Concrete

| Parameters for the Damage Model for massive concrete |                     |                            |      |
|--|---------------------|----------------------------|------|
| Parameters   | Notation            | Value                      | Unit |
| Young modulus  | $E$                 | 35000                      | MPa  |
| Poisson's ratio                                      | $\nu$               | 0.27                       | ---  |
| Tensile strength                                     | $R_t$               | 3.5                        | MPa  |
| Strain at $R_t$                                      | $\epsilon^{peak^t}$ | $1.0 \times \frac{R_t}{E}$ | ---  |
| Fracture energy in tension                           | $G_f^t$             | 1.37e-4                    | MN/m |
| Compressive strength                                 | $R_c$               | 45                         | MPa  |
| -strain at $R_c$                                     | $\epsilon^{peak^c}$ | 2.18e-3                    | ---  |
| Drucker-Prager Parameter                             | $\delta$            | 0.15                       | ---  |
| Fracture energy in compression                       | $G_f^c$             | 1.372e-2                   | MN/m |

Table 2. Model Parameters for Interface Bond Element

| Parameters for interface bond element behaviour law as 'elastic-plastic isotropic' |                            |        |      |
|--|----------------------------|--------|------|
| Parameters   | Notation                   | Value  | Unit |
| Young modulus  | $E$                        | 7298.2 | MPa  |
| Poisson's ratio  | $\nu$                      | 0.27   | ---  |
| Stress-strain curve  | Obtained from Pullout Test |        |      |

Table 3. Parameters for the Model of Steel Bar

| Parameters for steel bars behaviour law as 'elastic-plastic perfect' |          |            |                |
|--|----------|------------|----------------|
| Parameters   | Notation | Value      | Unit           |
| Young modulus  | $E$      | 195000     | MPa            |
| Poisson's ratio  | $\nu$    | 0.27       | ---            |
| Cross sectional area   | $A_s$    | 0.00011309 | m <sup>2</sup> |
| Yielding strength  | $f_y$    | 510        | MPa            |

This figure shows the ability of the approach adopted to model the interface between steel reinforcement and concrete matrix as

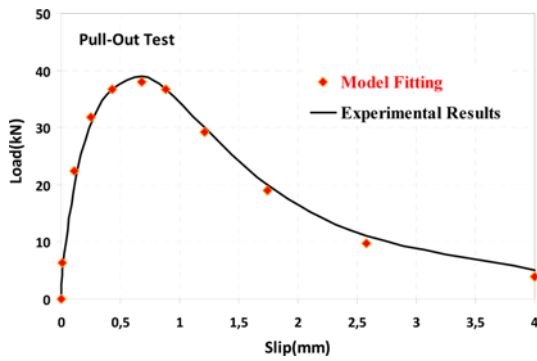


Fig. 7. Pull-out Test Simulation Result (model fitting)

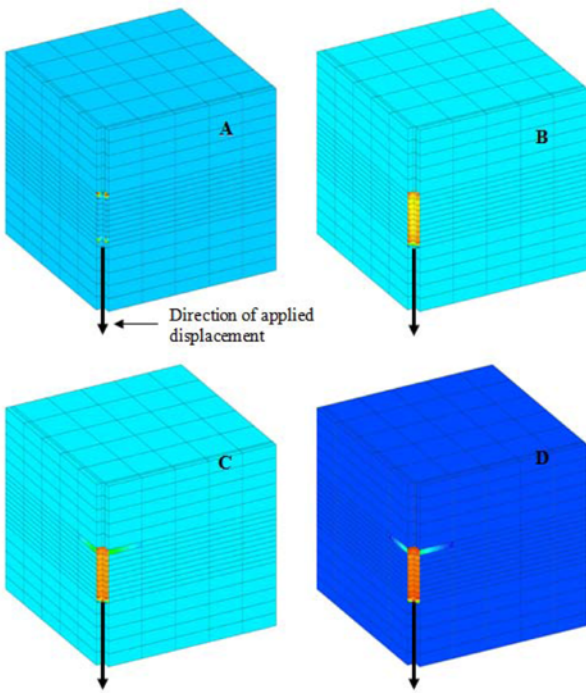


Fig. 8. Damage Evolution in Concrete in Pullout Test

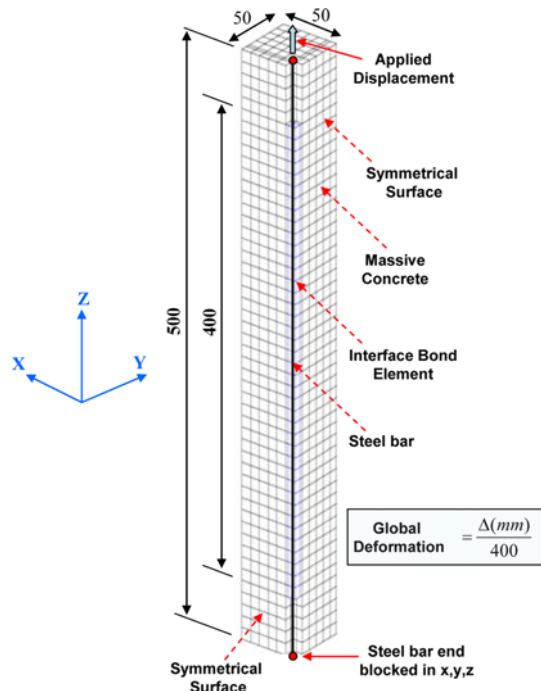


Fig. 9. 3D Finite Element Mesh of one Fourth of Element Subjected to Pure Tension

used to simulate pullout test which have been listed in Table 1 to Table 3.

To perform calculation in case of pure tension test the ‘mean shear stress’ deduced from pull-out test results has to be reduced by an empirical factor (close to 0.5). Without this reduction, the shear stress in tensile test is systematically over estimated leading to too many localized cracks. The need of this reduction factor is certainly due to the fact that in pure tension test, the shear stress distribution along the steel bar between two consecutive cracks is quite different from shear stress distribution in pull out test. Moreover, the assumption of homogeneous shear stress used to model the pull-out test is

the model predict quite well the load-slip response in the pullout test simulation.

Damage evolution in the finite element mesh of massive concrete at the contact surface with the steel bar is shown in Fig. 8, where progressive damage with the increase of steel bar slip can be observed.

### 3.2 Model Validation: RC Element Subjected to Pure Tension

Once the proposed interface element was fitted on pullout tests, it was tested on reinforced concrete element subjected to pure axial tensile loading. Three dimensional finite element mesh of the one fourth of the specimen is shown in Fig. 9 along with all necessary details about the size of the specimen, boundary conditions and loading point. The values of different parameters for the behaviour laws for the massive concrete, steel bar and interface bond element are the same as

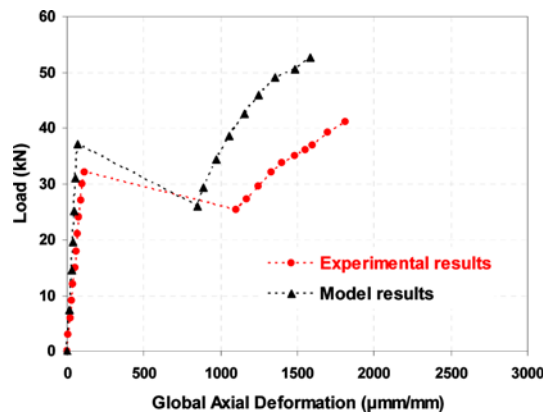


Fig. 10. Comparison of Load Versus Global Axial Deformation Curves (model and experiment results – RC prism subjected to pure tension)

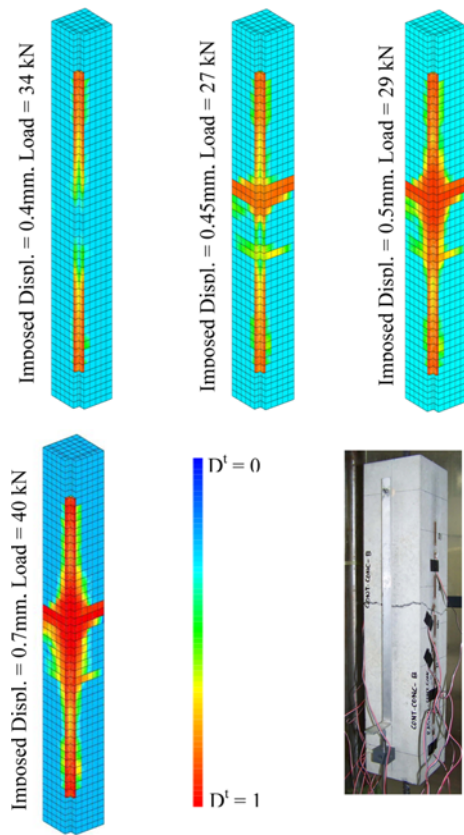


Fig. 11. Computed Damage Pattern and Experimental Crack Pattern

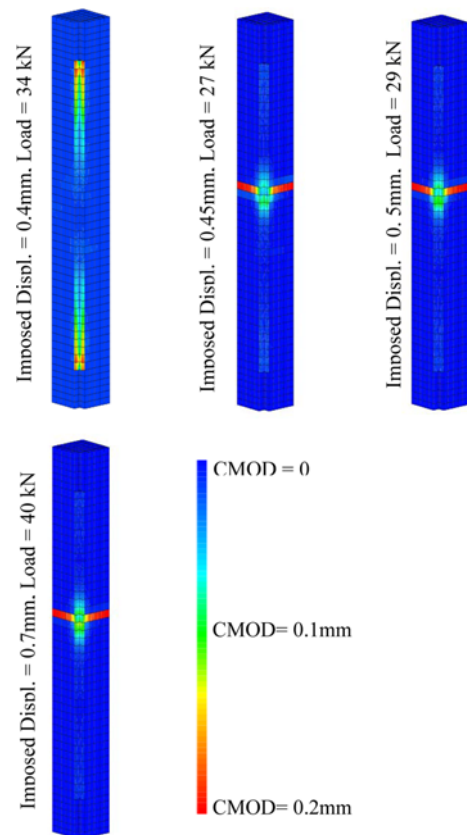


Fig. 12. Computed Crack Opening

also an approximation. To finely understand the problem, resorting to a mesoscopic approach (LaBorderie *et al.*, 2010) of local behaviour of the interface could be interesting, but this is not the object of our work which focuses on an efficient macroscopic approach to obtain realistic crack pattern at structure scale.

From the numerical simulation of the problem in finite element code CASTEM, global axial deformation versus load curve obtained from the modelling and crack localisation in the finite element mesh has been compared with the experimental results. Comparison of the experimental and model curves is presented in Fig. 10.

In the Fig. 11, localized crack and damage evolution in the finite element mesh of the test specimen is shown, where some diffusion of the damage in the neighbouring element to the localized crack is also observed in the last mesh with well localised crack. This shows that concrete on the two sides of the crack is not fully unloaded and contribute to carry minor stress along with the steel bar. The CMOD evolution is shown in Fig. 12. It is obvious in this figure that the computed position of the localised crack is similar to that of observed experimentally as shown in Fig. 11.

### 3.3 Model Validation: Reinforced Concrete Beam

In this section, the proposed method to model the interface

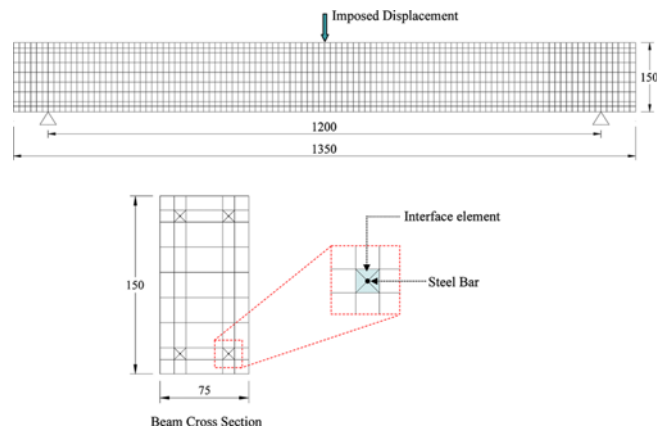


Fig. 13. Finite Element Mesh of Reinforced Concrete Beam

between steel bar and concrete is used to simulate the behaviour of reinforced concrete beam. Finite element meshing of RC beam in CASTEM is shown in Fig. 13. Span length and cross-sectional dimension of test specimen (beam) are also given in the same figure along with geometrical details of interface element. Reinforcement detail of test specimen is given in Fig. 14. The bar element corresponding to the main steel reinforcement (modelled as elastic perfectly plastic) and the cubic elastic plastic element representing the interface between concrete and steel bar are also shown in Fig. 14. Shear reinforcing bars (stirrups) were modelled as bar element with elastic perfectly plastic behaviour. In the

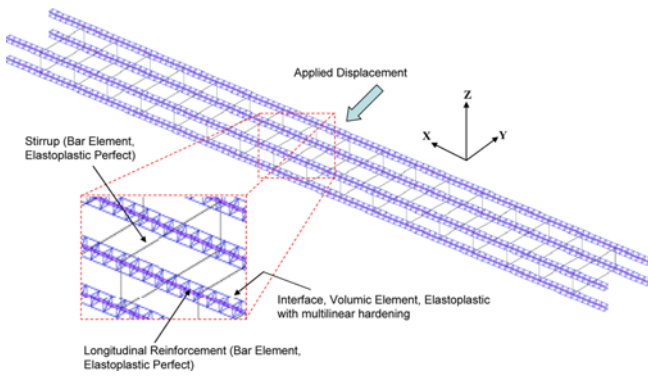


Fig. 14. Reinforcement and Interface

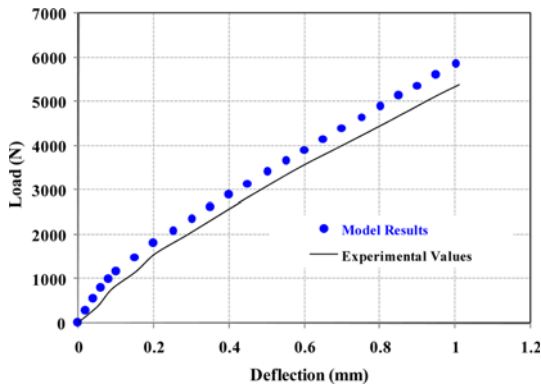


Fig. 15. Comparison of Experimental and Computed Load-deflection Curves

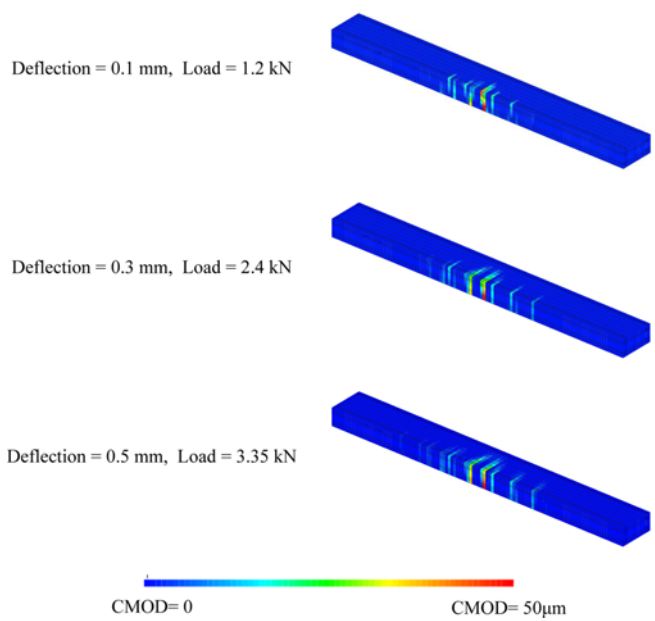


Fig. 17. Finite Element Mesh of Reinforced Concrete Beam

model, the loading was applied through an imposed vertical displacement in the mid span. Fig. 15 shows the load-deflection curves and allows comparison of computed values with the experimental values. Fig. 16 and Fig. 17 show the model ability to capture damage and to compute CMOD.

#### 4. Conclusions

A simplified approach to model steel-concrete interface in reinforced concrete structures has been proposed in this contribution. Interface between steel rebar and concrete is modelled using volumic element with elasto-plastic multi-linear hardening behaviour. Stress-strain curve required for interface bond element in RC is obtained from experimental pull-out test results modified by a reduction coefficient of 0.5 to account for the difference in shear stress distribution along the steel bar in pull out test specimen and in other RC elements. The ability of proposed approach to model steel-concrete interface has been illustrated by testing it in simulating behaviour of RC prism subjected to pure tensile loading and RC beam in flexure. Simulation results indicated good agreement with experimental observations. The simplicity of the simulation approach lies in the fact that all model parameters have definite physical meanings and their values may be determined by performing some classical tests on concrete and steel specimens.

#### Acknowledgements

The authors acknowledge the financial support of Higher Education Commission (HEC) of Pakistan for this work. We are also grateful to CEA/DEN/DM2S/SEMT for providing the finite element code CASTEM.

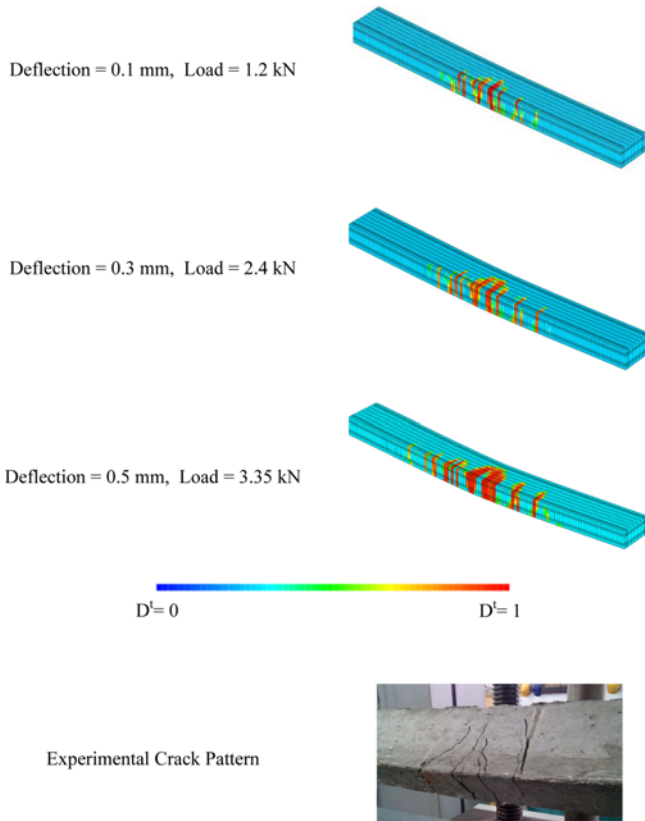


Fig. 16. Computed Damage Pattern and Experimental Crack Pattern

## Notations

- $A_c$  = Area of massive concrete  
 $E_c$  = Elastic modulus of massive concrete  
 $A_s$  = Cross-sectional area of steel reinforcing bar  
 $E_s$  = Elastic modulus of steel  
 $A_i$  = Cross-sectional area of interface element  
 $E_i$  = Elastic modulus of interface element  
 $d_b$  = Diameter of bar  
 $K_o$  = Global stiffness  
 $D_t$  = Tensile damage tensor  
 $\mathcal{D}^c$  = Compressive damage tensor  
 $\mathcal{S}^0$  = Stiffness matrix of the un-damaged concrete  
 $\vec{\sigma}^e$  = Effective Stress  
 $\vec{\sigma}^c$  = Negative effective Stress  
 $\vec{\sigma}^t$  = Positive effective Stress  
 $\vec{\epsilon}$  = Total strain  
 $\vec{\epsilon}^p$  = Plastic strain  
 $\vec{\epsilon}^t$  = Tensile plastic strain  
 $\vec{\epsilon}^c$  = Compression/shear plastic strain  
 $G_f$  = Fracture energy

## References

- Casanova, J., Jason, L., and Davenne, L. (2012). "Bond slip model for the simulation of reinforced concrete structures." *Engineering Structures*, Vol. 39, pp. 66-78, DOI: 10.1016/j.engstruct.2012.02.007.
- CAST3M (2000). Finite element software. Commissariat à l'Énergie Atomique, <http://www-cast3m.cea.fr>
- Dominguez, N. and Ibrahimbegovic, A. (2006). "A non-linear thermodynamical model for steel-concrete bonding." *Computers and Structures*, Vols. 106-107, pp. 29-45, DOI:10.1016/j.compstruc.2012.04.005.
- Guo, J. and Cox, J. V. (2000). "Implementation of a plasticity bond model for reinforced concrete." *Computers and Structures*, Vol. 77, pp. 65-82, DOI: 10.1016/S0045-7949(99)00196-0.
- Jendele, L. and Cervenka, J. (2006). "Finite element modelling of reinforcement with bond." *Computers and Structures*, Vol. 84, pp. 1780-1791, DOI: 10.1016/j.compstruc.2006.04.010.
- LaBorderie, C., Lawrence, C., N'Guyen, T. D., and Nahas, G. (2010). "A mesoscopic approach for a better understanding of the transition from diffuse damage to localized damage." *Fracture mechanics of concrete and concrete structures, recent advances in fracture mechanics of concrete*, edited by B.H. Oh et al., Korea Concrete Institute, ISBN 978-89-5708-180-8.
- Mang, C., Jason, L., and Davenne, L. (2015). "A new bond slip model for reinforced concrete structures: validation by modelling a reinforced concrete tie." *Engineering Computation*, Vol. 32 No. 7, pp.1934-1958.
- Mazzarolo, E., Scotta, R., Berto L., and Saelta, A. (2012). "Long anchorage bond-slip formulation for modelling of r.c element and joints." *Engineering Structures*, Vol. 34, pp. 330-341, DOI: 10.1016/j.engstruct.2011.09.005.
- Ngo, D. and Scordelis, A. C. (1967). "Finite element analysis of reinforced concrete beam." *ACI Journal*, Vol. 64, pp. 152-63, DOI: 10.14359/7551.
- Pyo, S. H. and Lee, H. K. (2010). "An elastoplastic damage model for metal matrix composites considering progressive imperfect interface under transverse loading." *International Journal of Plasticity*, Vol. 26, pp. 25-4, DOI: 10.1016/j.ijplas.2009.04.004.
- Radtke, F. K. F., Simone, A., and Sluys, L. J. (2010). "A computational model for the failure analysis of fibre reinforced concrete with the discrete treatment of fibres." *Engineering Fracture Mechanics*, Vol. 77, pp. 597-620, DOI: 10.1016/j.engfracmech.2009.11.014.
- Ragueneau, F., Dominguez, N., and Ibrahimbegovic, A. (2006). "Thermodynamic-based interface model for cohesive brittle materials: Application to bond slip in RC structures." *Computer Methods in Applied Mechanics and Engineering*, Vol. 195, pp. 7249-7263, DOI: 10.1016/j.cma.2005.04.022.
- RILEM 7-II-128 (1994). "RC6: Bond Test for Reinforcing Steel. Pull-Out Test." *RILEM Technical Recommendations for the Testing and use of Construction Materials*, E & FN Spon, U.K. pp.102-105.
- Sellier, A. (2015). *Model FLUENDO3D Version 20-P for Castem 2012, Tentative Handbook, Laboratoire Matériaux et Durabilité des Constructions (LMDC) Internal Document*, Toulouse, France. Retrieved from [alain.sellier@insa-toulouse.fr](mailto:alain.sellier@insa-toulouse.fr)
- Sellier, A., Casaux-Ginestet, G., Buffo-Lacarrière, L., and Bourbon, X. (2010a). "Orthotropic damage coupled with localised crack reclosure processing. Part I: Constitutive laws." *Engineering Fracture Mechanics*, Vol. 97, pp. 148-167, DOI: 10.1016/j.engfracmech.2012.10.012.
- Sellier, A., Casaux-Ginestet, G., Buffo-Lacarrière, L., and Bourbon, X. (2010b). "Orthotropic damage coupled with Localized crack reclosure processing. Part II: Applications." *Engineering Fracture Mechanics*, Vol. 97, pp. 168-185, DOI: 10.1016/j.engfracmech.2012.10.012.
- Wang, X. and Liu, X. (2003). "A strain-softening model for steel-concrete bond." *Cement and Concrete Research*, Vol. 33, pp. 1669-1673, DOI: 10.1016/S0008-8846(03)00137-6.
- Willam, K., Rhee, I., and Shing, B. (2004). "Interface damage model for thermomechanical degradation of heterogeneous materials." *Computer Methods in Applied Mechanics and Engineering*, Vol. 193, pp. 3327-3350, DOI: 10.1016/j.cma.2003.09.020.